Microbeam Analysis, 3 (1994) 211-224

New Developments in Electron Probe Microanalysis of Oxygen in Wide Bandgap Oxides

M. Fialin*
URA 736 CNRS, Université Pierre et Marie Curie, 75252 Paris Cedex 05, France

G. Remond
Département Géologie, Bureau de Recherches Géologiques et Minières, BP 6009, 45060 Orléans Cedex 2, France

C. Bonnelle
Laboratoire de Chimie Physique Matière et Rayonnement, Université Pierre et Marie Curie-URA 176 CNRS, 11 rue Pierre et Marie Curie, 75321 Paris Cedex 05, France
Received: December 22, 1993

ABSTRACT

The Kα intensity emitted from low-Z atoms in solids depends on the density of occupied valence states on the emitting atom sites (partial DOS). For oxygen, the O Kα peak reflects the band structure of the partial O DOS with p symmetry of the emitting solid. The chemical bonding in oxides for O atoms ranges widely from pure ionic (e.g., Cu_2O) to rather covalent (e.g., SiO_2). The more intense peaks are expected for ionic oxides, which correspond to both strong electron transfers from neighboring cations to O atoms and narrow DOS in energy. In other words, the rate of generated O Kα photons per atom is strongly dependent on the chemical nature of oxides. As a direct consequence of this statement, electron probe microanalysis (EPMA) should be regarded as an inappropriate method for quantitative analysis of oxygen. Nevertheless, accurate results are obtained if a relationship exists between both the position and the shape of the O Kα peak, as resolved by monochromators with high enough resolving powers, such as TAP crystals. The shake-off peaks (satellite emissions resulting from multiply ionized atoms) strongly contribute to the total O K emission band and play an important role in the regulation of the O Kα intensity from one oxide to another. Most O Kα peaks emitted from semiconducting oxides satisfy the relationship previously mentioned. On the other hand, the O Kα peaks emitted from wide bandgap oxides, such as those in the MgO-Al_2O_3-SiO_2 system, are generally narrow compared to semiconductor peaks, leading to overestimated EPMA results. Moreover, radiative recombinations of states located in the specimen bandgap increase the fluorescence yield of O atoms in wide bandgap oxides. These parasite de-excitation processes of oxygen atoms are related to a peak, Kα'', located on the high-energy side of O Kα. For Al_2O_3, Kα'' is estimated to 7% of Kα and should be ignored for the k-ratio measurements.

*To whom correspondence should be addressed.
Centre d'Analyses par Microsonde-UPMC Tour 26-3ème étage-4, place Jussieu—75252 Paris Cedex 05-France
Phone: (33) 44.27.39.10; Fax: (33) 44.27.39.11

1061-3420/94/$5.00 + .25

KEY WORDS: *Electron probe microanalysis of oxygen, radiative transition probability, fluorescence yield, radiative recombination of bandgap states, ionic and covalent oxides, shake-off peaks.*

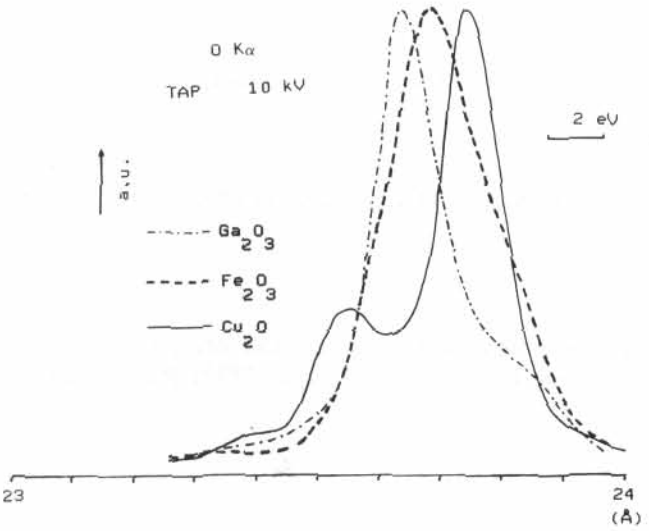

FIGURE 1. Oxygen emission lines from Ga_2O_3, Fe_2O_3, and Cu_2O, using a TAP monochromator.

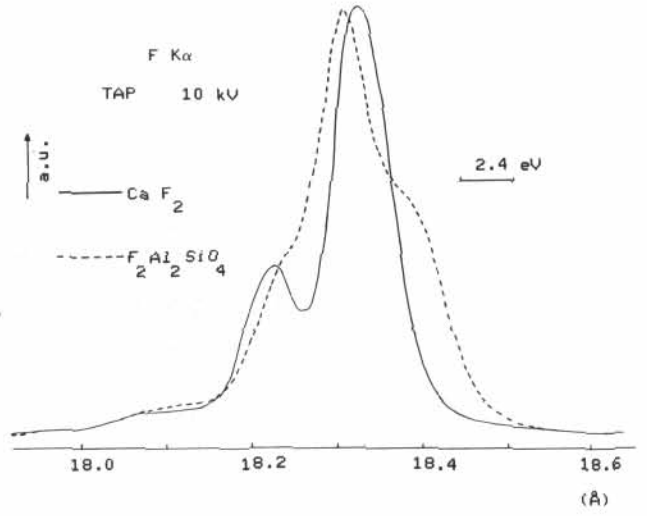

FIGURE 2. Fluorine emission lines from CaF_2 (fluorite) and $F_2Al_2SiO_4$ (topaz).

1. INTRODUCTION

The probability P_{if} for a radiative transition between two levels i and f of an atomic species in a material can be expressed through time-dependent perturbation theory and the independent-electron approximation (Koopmans approximation). The general relationship is as follows (Bonnelle, 1987):

$$P_{if} = W_{if} \cdot \tau_i \cdot N_i \tag{1}$$

where W_{if} is the probability per time unit for a spontaneous emission $h\nu_{if}$, which is proportional to the product $h\nu_{if}^3 \cdot r_{if}^2$. The term $r_{if} = \langle \psi_f | r | \psi_i \rangle$ is known as the dipolar matrix element of the transition, where ψ_i and ψ_f are the wave functions that describe the electron, respectively, in the states i and f, and r is the position of the electron. For $2_p \rightarrow 1s$ transitions (Kα emissions), W_{if} is proportional to Z^4 (Z-atomic number). The term τ_i is the lifetime of the vacancy in the initial state i. τ_i is related to the natural width ΔE_i of the i level by the Heisenberg's uncertainty principle: $\Delta E_i \cdot \tau_i \sim h$. The term N_i is the number of atoms in the initial level i, per unit volume (to be consistent, P_{if} is a probability per unit volume).

The product $W_{if} \cdot \tau_i$ can be expressed under a more familiar form for microanalysts:

$$W_{if} \cdot \tau_i = \omega_i \cdot z_{if} \tag{2}$$

where ω_i is the fluorescence yield (i.e., the sum of the probabilities of all radiative transitions divided by the sum of the probabilities of all radiative and nonradiative (Auger) transitions involving the i level). The term z_{if} is the parameter known as weight of the line (i.e., the proportion of emitted $h\nu_{if}$ photons compared to all radiative transitions involving the i level). Further theoretical developments concerning transition probability for radiative transitions can be found in Feldman and Mayer (1986).

The intensity I_{if} in the radiative transition is proportional to P_{if} and depends on the convolution of the two levels' energy distribution, D_i and D_f

$$I_{if} \propto P_{if} \cdot D_i^* D_f = P_{if} \cdot D_{if} \tag{3}$$

For transitions between two core (atomic) levels, D_{if} is generally considered as being independent of the environment of the emitting atom. Consequently, D_{if} is not taken into account in matrix-correction models, at least for EPMA with standards. The value of D_{if} is assumed to be unchanged in both the unknown and the standard.

On the other hand, light-element EPMA involves transitions from the valence band of analyzed compounds. In that case, the distribution of valence electrons D_f upon a given atomic site, also called local or partial density of occupied states (DOS), can no longer be taken as a constant. Indeed, this distribution may change according to the chemical bond strength with surrounding

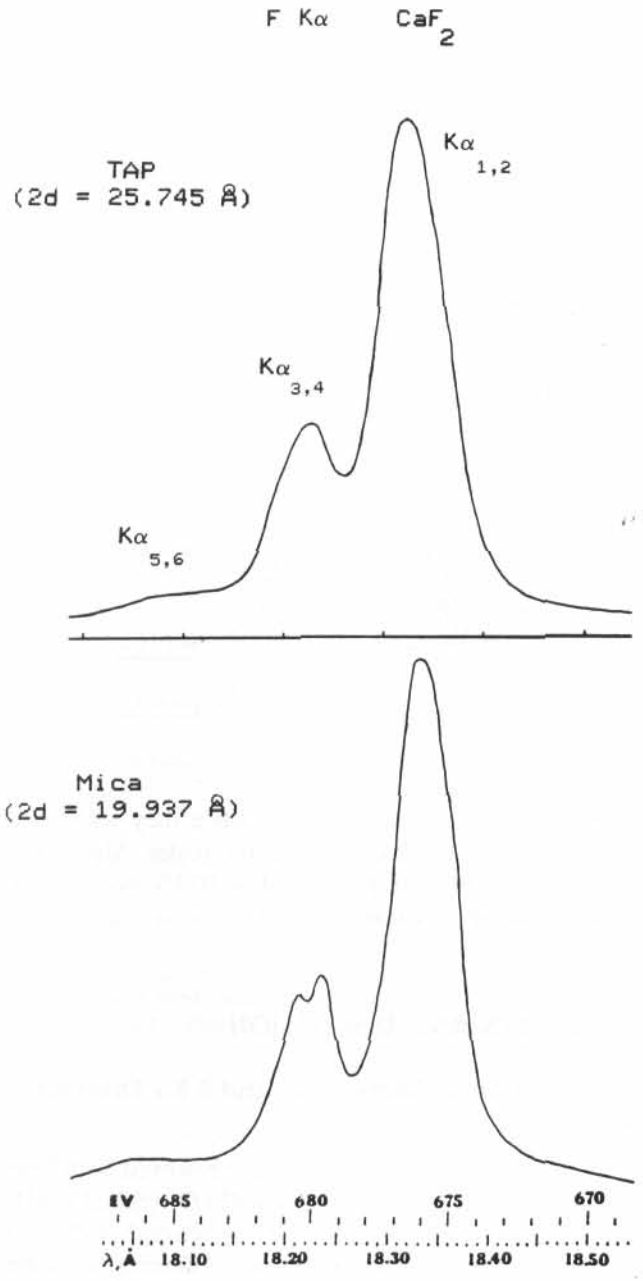

FIGURE 3. Fluorine emission lines from CaF_2. The improved resolution is obtained with the mica monochromator, showing that shake-off peak $K\alpha_{3,4}$ is a doublet.

partners. Any change in the chemical environment of the element will involve a spatial redistribution of the valence electrons. Changes in DOS affect not only both the natural widths and binding energies of the valence levels, but also those of the core levels. These changes are the reason for the peak shifts and peak-shape alterations, known as chemical effects in EPMA, that are observed on soft radiations emitted from different specimens. The consequences of chemical effects on EPMA have been fully discussed by Bastin and Heijligers (1985, 1986, 1989, 1991) in connection with the building of their light-element databases.

More important for our purpose is the influence of the changes in DOS on the intensity I_{if}. Two points must be examined:

1. The matrix element r_{if} depends on the overlap between ψ_i and ψ_f in such a way that the probability W_{if} increase with the amount of overlap. Thus, the most intense transitions are those occurring between core levels. For transitions between the valence band and a highly localized core hole, only the amplitude of ψ_f in the region of the core contributes to the transition matrix element.
2. As has been previously suggested, the local DOS influences I_{if} directly through the parameter D_f in Equation 3. It is well known that the transfer of valence electrons between two atoms that are chemically bonded is directed towards the more electronegative of the two: the larger the charge transfer, the stronger the ionic character of the bond. In oxides, for instance, this transfer occurs from cations to oxygen atoms. Charge transfers influence D_f directly.

Consequences of the preceding point on oxygen EPMA already have been discussed in a recent article (Fialin and Remond, 1993). The present study is designed to provide further arguments to consider EPMA failure in certain light-element problems through the description of emission-band properties. This approach asks the crucial question for EPMA: is the basic physical information, the rate of photons generated per ionized atom of the analyzed species, identical for the unknown and for the standard? On the other hand, the usual tendency is for the microanalyst to systematically suspect the matrix-correction models every time an analytical problem occurs; results are incorrect, hence the correction models have failed. Our purpose is to pursue a careful investigation of the O $K\alpha$ emission bands emitted from many oxides. Particular attention is paid to the origin of the O $K\alpha$ components. The behavior of some $K\alpha$ emission bands emitted from neighboring elements (fluorine and boron) is examined for comparison.

2. MATERIALS AND METHODS

Electron probe microanalysis as well as peak profiles presented in this paper have been performed on four CAMECA microprobes (Camebax Microbeam and SX50 types) equipped with W/Si ($2d$ spacing of 6 nm) and Ni/C ($2d$ spacing of 9.5 nm) multilayers and lead stearate crystals ($2d$ spacing of 10 nm) as monochromators for oxygen measurements. The additional spectra shown (F $K\alpha$ and Al $K\beta$) have been recorded using TAP crystals ($2d$ spacing of 2.575 nm). Two of these microprobes

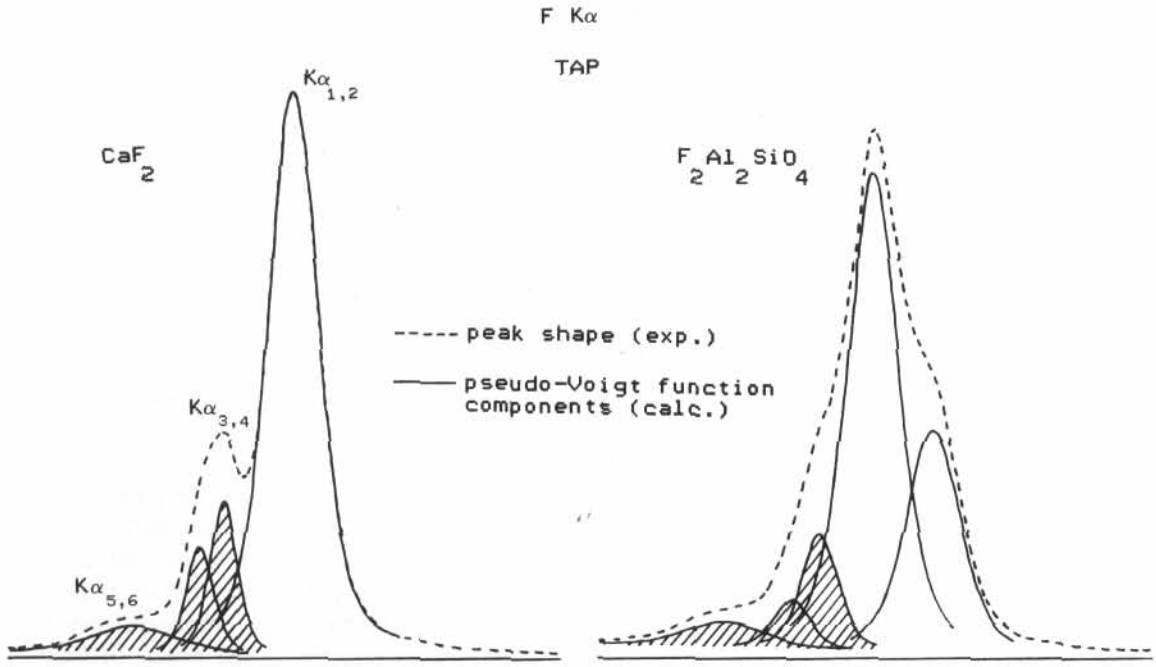

FIGURE 4. *Decomposition into pseudo-Voigt functions of the fluorine spectra from Figure 2.*

are installed at the joint BRGM-CNRS microanalysis laboratory in Orléans and two are at the CAMPARIS microanalysis center in Paris.

O Kα peak profiles as resolved by a TAP crystal were recorded by means of a special spectrometer, with improved mechanical limits compared to conventional spectrometers, in order to scan high Bragg-angle regions (upper limit: sin θ = .93300). These measurements were performed at the CAMECA's application laboratory in Courbevoie. Electron probe microanalysis results were obtained with a quantitative analysis program that is particularly well adapted to the processing of light-element data and which has been recently presented (Fialin *et al.*, 1993).

Some peaks were mathematically decomposed into pseudo-Voigt components (a linear combination of gaussian and lorentzian functions) after the digitally recorded *spectra were treated by a fitting program described elsewhere* (Remond *et al.*, 1989).

All strongly insulating oxides used for this study were made conductive by coating them with a carbon film 15 to 20 nm thick. The Al_2O_3 samples were either natural species (corundum, sapphire) or one synthetic single crystal (α–Al_2O_3 cut to the (1012) orientation plane). The MgO sample was a natural crystal (periclase); BeO was synthetic, obtained by the sintering of grains between 10 to 30 μm in dimension.

One CaF_2 (fluorite) and one $F_2Al_2SiO_4$ (topaz) natural crystal were carbon coated and used for fluorine measurements: Conducting oxides, Ga_2O_3 (a synthetic single crystal), Fe_2O_3 (a natural hematite), and Cu_2O (a natural cuprite) were carbon coated only when they were used as standards for EPMA of insulating oxides. Most spectra reported here were performed at 10 kV accelerating voltage and 100 nA beam current.

3. RESULTS AND DISCUSSION

A Description of Some O Kα and F Kα Emission Bands

Figure 1 shows typical O Kα peaks, resolved by a TAP monochromator and emitted from Ga_2O_3 (called Ga_2O_3 spectrum in the text), Fe_2O_3 (Fe_2O_3 spectrum), and Cu_2O (Cu_2O spectrum). *These spectra are representative of the* three classes of O Kα peaks according to Fisher (1965). The Cu_2O spectrum shows a main peak with two high-energy satellites at +4 eV and +7.5 eV. *The* Ga_2O_3 spectrum shows a low-energy structure at proximately −3 eV from the main peak whose the position is shifted by +2.4 eV from the Cu_2O spectrum maximum. High-energy satellites are no longer observable. The Fe_2O_3 spectrum is broad and no prominent structure is noted. Its maximum is shifted by +1.3 eV from the Cu_2O peak.

Both F Kα spectra plotted in Figure 2 using a TAP monochromator give the opportunity to make an interesting comparison with two O Kα spectra from Figure 1. Indeed, the CaF_2 spectrum shows obvious similarities with the Cu_2O spectrum. The same is true for both the $F_2Al_2SiO_4$ (topaz) and Fe_2O_3 spectra. Fluorine is chemically very close to oxygen and their Kα peaks can be

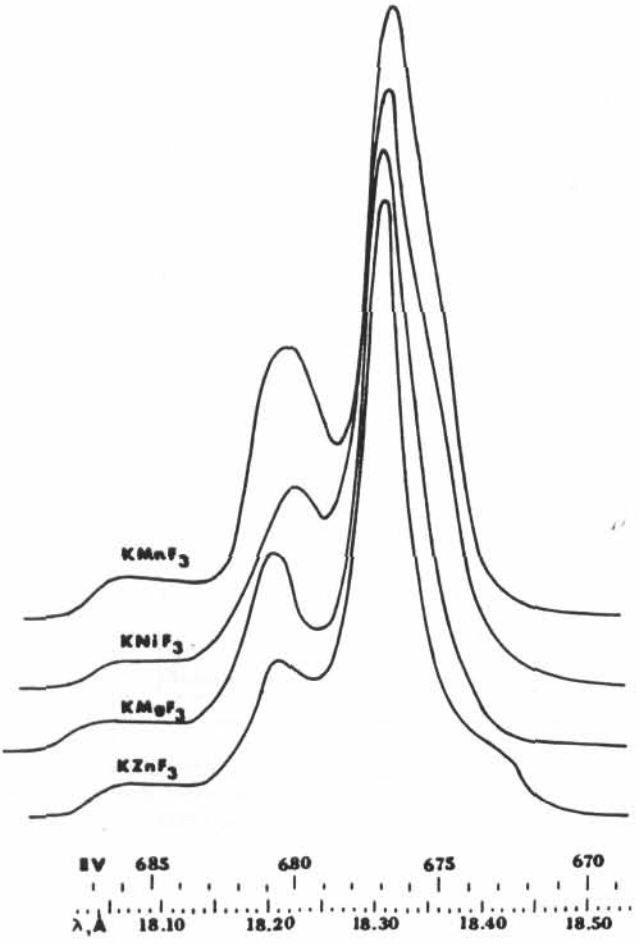

FIGURE 5. Fluorine emission lines from cubic fluorides ($CaTiO_2$ type), using a bent mica monochromator (reprinted from Mattson and Ehlert, 1966).

compared in many respects. Moreover, F Kα is higher in energy than O Kα, which allows for the use of monochromators with lower $2d$ spacings than TAP.

Two CaF_2 spectra, resolved by a TAP and a mica (Mattson and Ehlert, 1966) monochromator are compared in Figure 3. The better resolution is obtained with the mica (2d spacing of 1.99 nm) and shows that the high-energy satellite labelled K$\alpha_{3,4}$ at +3.4 eV from the main peak K$\alpha_{1,2}$ is a doublet. As has been previously mentioned (Fialin *et al.*, 1993) K$\alpha_{3,4}$ corresponds to the radiative de-excitation of F^- ions in the presence of one vacancy in the L level, created at the same time as the initial K vacancy. The atom is thus initially doubly ionized, leading to $KL_{2,3} \rightarrow L^2_{2,3}$ transitions. K$\alpha_{5,6}$ at +8.8 eV from K$\alpha_{1,2}$ is due to a second L vacancy (K $(L_{2,3})^2 \rightarrow (L_{2,3})^3$ transitions) K$\alpha_{3,4}$ and K$\alpha_{5,6}$ are known as shake-off peaks.

The next step consists in looking at the evolution of each of the Kα components (main-, high-, and low-energy peaks) when changing the emitting specimen. For that purpose, Figure 4 presents a decomposition into pseudo-Voigt functions of the F Kα spectra from Figure 2.

First, the CaF_2 spectrum was processed. Four pseudo-Voigt functions, composed of 40% gaussian—60% lorentzian, were chosen for this problem (one forK$\alpha_{1,2}$, one for K$\alpha_{5,6}$, and two for K$\alpha_{3,4}$). For each function, the gaussian and the lorentzian distribution was centered at the same position, with the same amplitude and full-width at half-maximum (FWHM). All components of the CaF_2 peak were well separated from each other, which facilitates the estimation of the initial parameters (maximum peak position, amplitude, and FWHM for each declared function) to be introduced in the fitting program. The positions of the K$\alpha_{3,4}$ doublet maxima have been deduced from Figure 3.

The calculated final parameters for this spectrum have then been used as the initial parameters for the processing of the topaz spectrum. An additional function, with the same FWHM as the main peak, has been introduced to take into account the low-energy peak. The topaz spectrum shows pronounced structures, unlike the Fe_2O_3 spectrum, which limit the degrees of freedom of the adaptable parameters (i.e., amplitude, FWHM, position) during the fit calculations.

Satisfying fits were obtained in both case. The main result concerns the changes in the intensity of the shake-off peaks in both specimens; the weight of these peaks is 25% of the total peak for CaF_2, reduced to 18% for topaz. A slight decrease of the K$\alpha_{1,2}$–K$\alpha_{3,4}$ distance was also noted, from 4.2 eV for CaF_2 to 3.4 eV for topaz.

The evolution of the F Kα peak emitted from some cubic fluorides of the same series ($CaTiO_2$ type) is examined in Figure 5 (Mattson and Elhert, 1966). A great advantage of these spectra is the good resolution obtained for the shake-off peaks over the fluoride series, leading to a direct observation of the aforementioned results in a mathematical way: the shake-off peaks' intensity decreases as the main peak shifts to high energies. Correlatively the K$\alpha_{1,2}$–K$\alpha_{3,4}$ distance tends to decrease. On the other hand, the energy of the low-energy peak decreases and becomes better resolved as the main peak energy increases.

Figure 6 illustrates for oxygen the general trends already observed for fluorine. Full-width at half-maximum vs. maximum position is plotted for O Kα peaks emitted from many binary oxides. These data were obtained either from our measurements using a TAP monochromator or from Fischer (1965) using a RbAP crystal with 2d spacing of 2.612 nm, close to 2.547 nm for TAP. Cu_2O has the less energetic and less narrow peak. As previously noted for the CaF_2 spectrum, the main K$\alpha_{1,2}$ emission band is composed of a single peak, and the shake-off peaks are well-resolved and contribute strongly to the total emission band. As the peak shifts to high energies, the FWHM increases, due to (1) the contribution of the low-energy satellite, whose the intensity increases, and

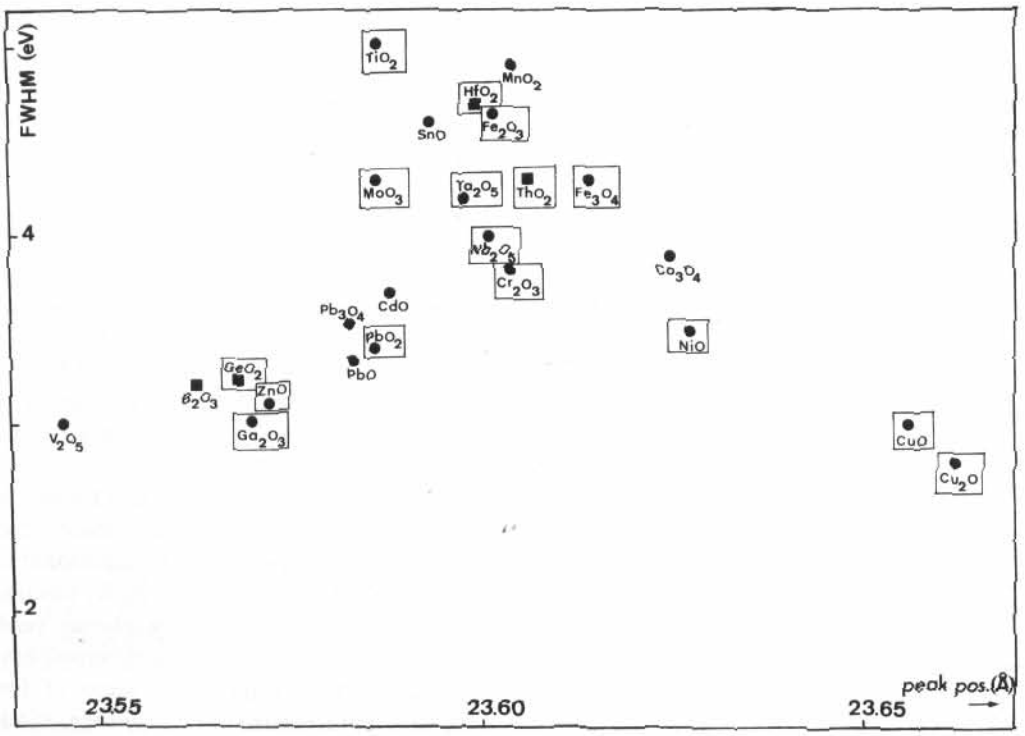

FIGURE 6. FWHM vs. maximum position plots for O Kα peaks from some binary oxydes. Spectra were recorded using TAP ($2d$ = 2.547 nm) or RbAP ($2d$ = 2.612 nm) monochromators. Circles = semiconducting oxides. Squares = insulating oxides. Boxed = oxides that have been checked to show no EPMA anomalies (our measurements and those by Bastin and Heijligers, 1989).

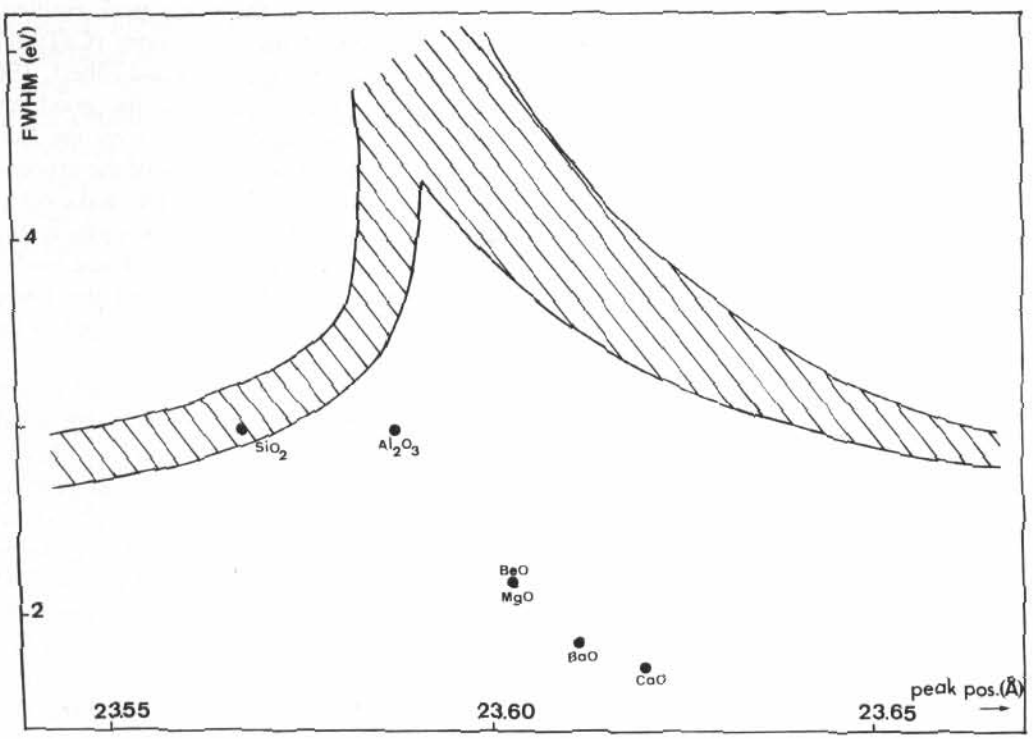

FIGURE 7. FWHM vs. maximum position plots for O Kα from some wide bandgap oxides. Hatched area corresponds to the region where plots from Figure 6 are located.

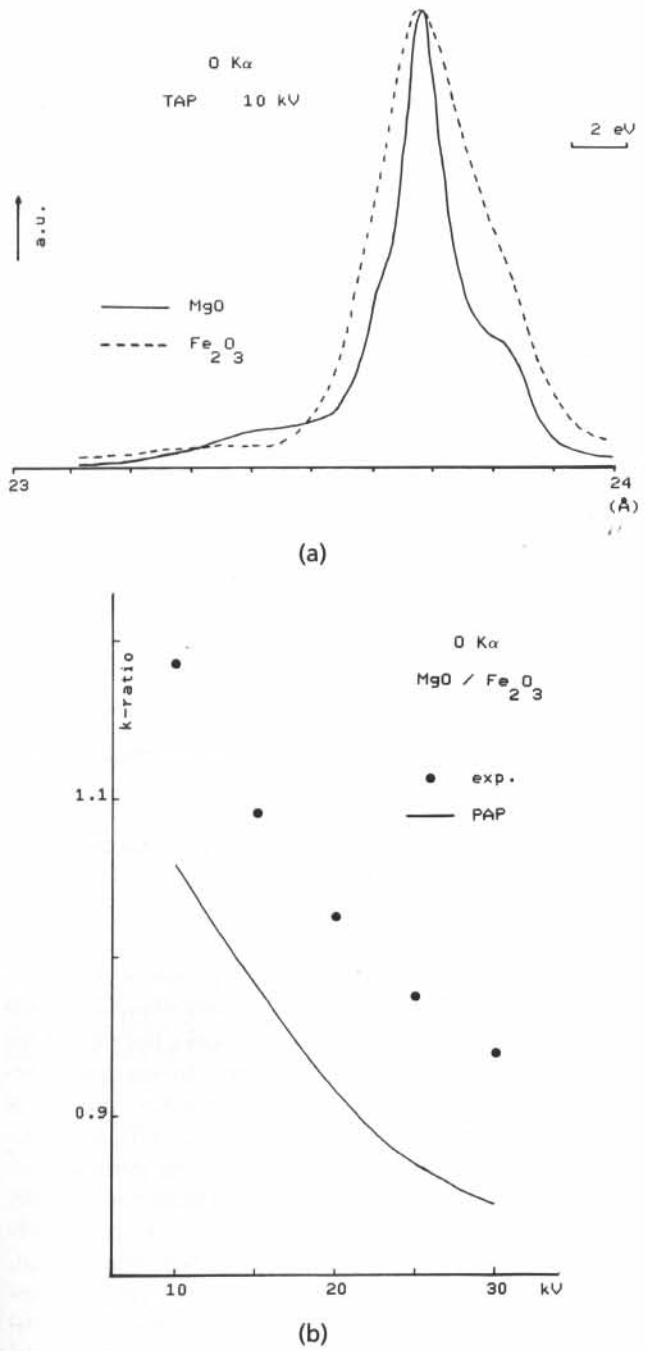

FIGURE 8. (a) Oxygen emission lines from MgO and Fe_2O_3. (b) O Kα *k*-ratios for MgO/Fe_2O_3. Mass-absorption coefficients from Henke *et al.*'s (1982) tables are used for calculations with the PAP model.

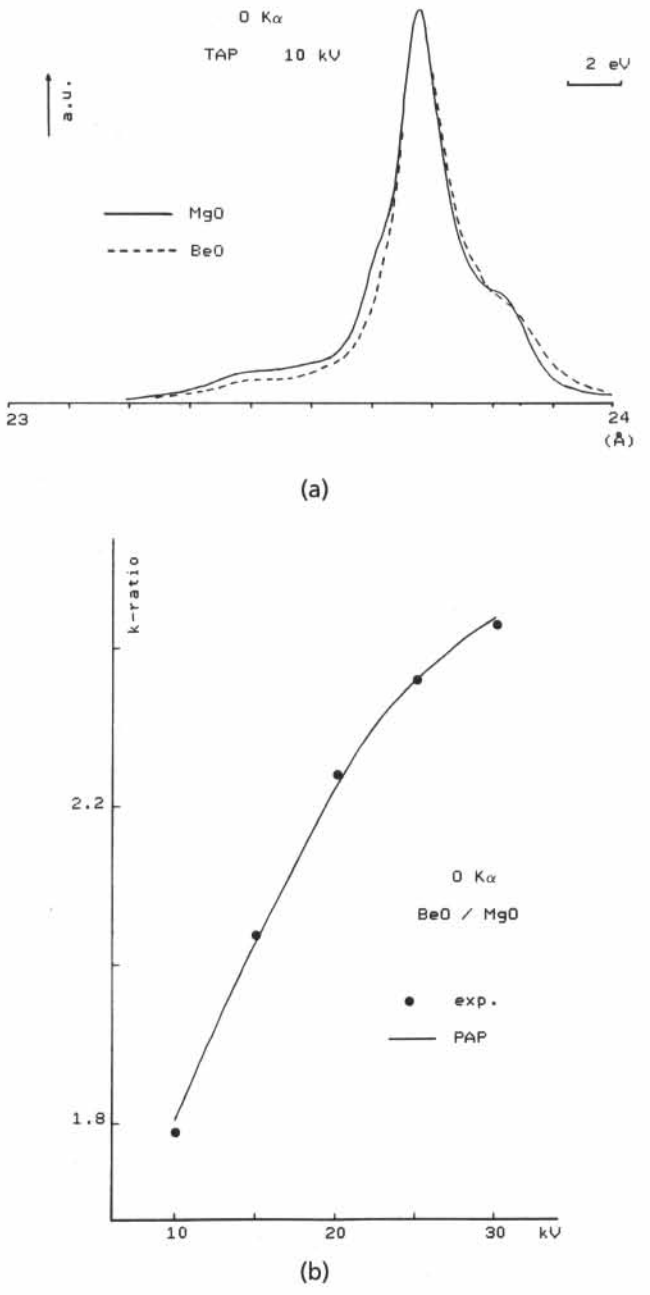

FIGURE 9. (a) Oxygen emission lines from MgO and BeO. (b) O Kα *k*-ratios for BeO/MgO (same remarks as Figure 8).

(2) the $K\alpha_{3,4}$–$K\alpha_{1,2}$ distance, which decreases at the same time. For wavelengths less than 2.359 nm, the FWHM decreases abruptly because the low-energy satellite separates by approximately 4 eV from the main peak and its contribution to the FWHM is weak. Moreover, the shake-off peaks are no longer observable. No strong evolution in shape is noted for peaks below 2.359 nm.

Role of the O Kα Peak Characteristics on the EPMA Anomalies

The important point to be emphasized is that no EPMA anomalies occur with the oxygen measurements for these oxides, regardless of electrical conductivity. This point must be discussed. According to Holliday (1968), the wavelength shift of a peak can be correlated with the number of electrons transferred from neighboring elements to the atom considered. One can conclude for oxides that the distribution of valence electrons present on

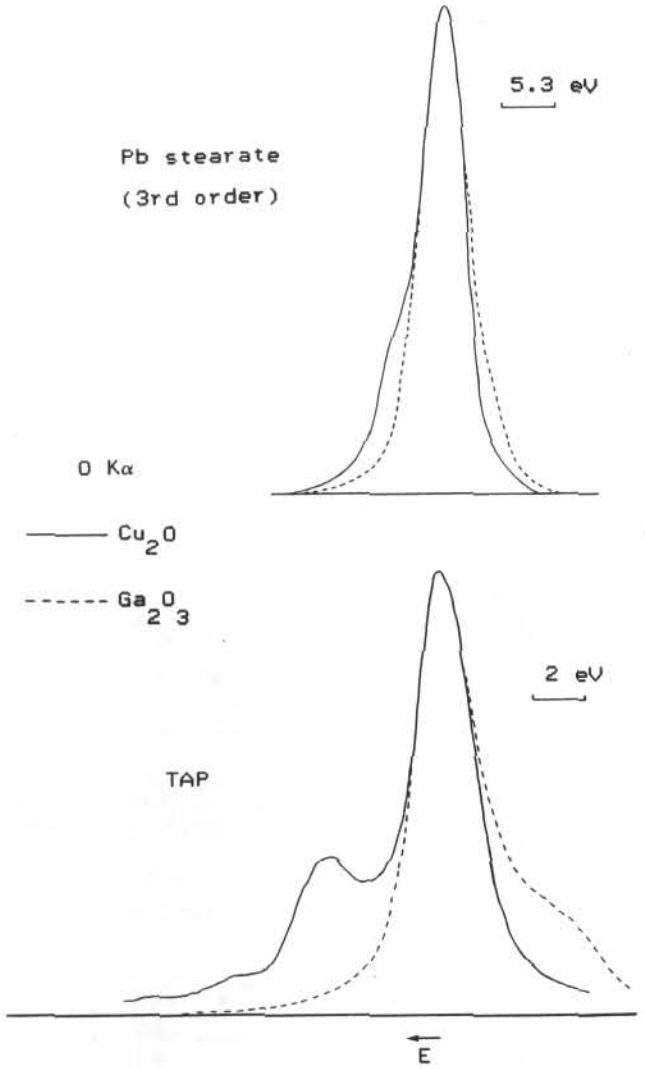

FIGURE 10. Comparison of the shapes of O Kα peaks from Cu_2O and Ga_2O_3, using lead stearate in the third order (top) and TAP (bottom). The two peaks were normalized to the same maximum intensity and then superimposed.

an oxygen atomic site varies over the wavelength range scanned in Figure 6. As a direct consequence of Equation 3, the parameter D_{if} must change at the same time. The question is, why are these changes not reflected as emission anomalies in EPMA? In our opinion, the role of the shake-off peaks must be considered.

Two points must be emphasized concerning these peaks: (1) These satellites may have a strong weight in the K peak for low-Z atoms. Indeed, the number of doubly ionized atoms may be as large as 20 to 30% (see Aberg (1967) for a theoretical justification of this point); and (2) The radiative recombination leading to a shake-off emission occurs in the presence of one or two extra vacancies in the L levels. Consequently, the parameter D_{if} is smaller for the shake-off peaks than for the related diagram peaks (main- and low-energy peak).

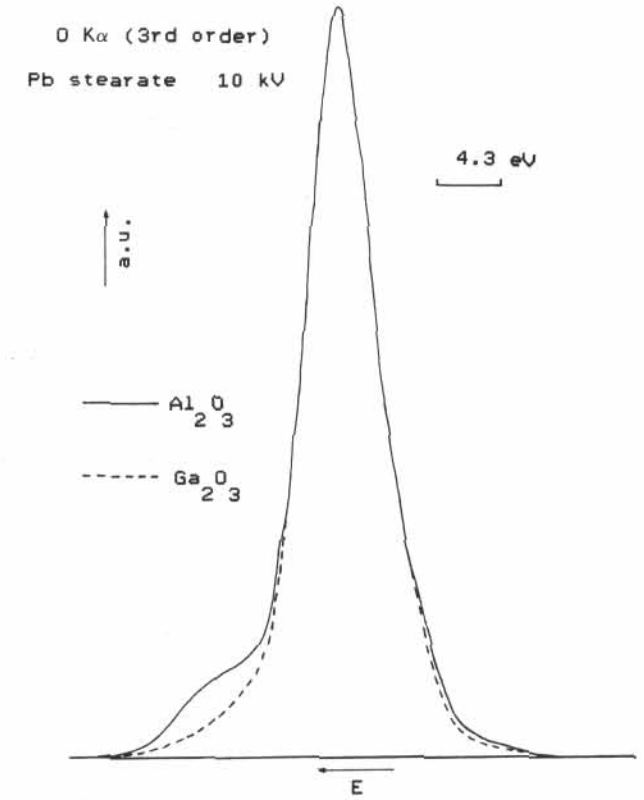

FIGURE 11. Comparison of the shapes of O Kα peaks from Al_2O_3 and Ga_2O_3 (lead stearate).

In our opinion, the poor emissive power of the shake-off peaks would balance, more or less completely, the excess in intensity for the diagram peaks because of the electron transfers on oxygen atoms. In summary, because of their strong contribution to the Kα emission of low-Z atoms, the shake-off peaks act as efficient regulators of bonding-induced changes in the generated intensity, a fact that renders EPMA applications possible.

The behavior of the shake-off peaks, described previously, provides further valuable information. Indeed, a decrease in the intensity of these peaks can be correlated with a decrease in the atomic character (i.e., a decrease in the electronic population), of valence levels. Schematically, the bonding is strongly ionic when the valence states are localized on the atom, whereas for a covalent bond, valence states are delocalized over at least two atoms. When, the shake-off peaks are important, the bonding is mostly ionic, as is the case for Cu_2O. As the main peak energy increases, fewer electrons are transferred on oxygen atoms (the covalent character in the bond is increasingly preponderant) as reflected in a gradual intensity loss of the shake-off peaks.

The FWHM vs. peak-position plots for some large bandgap simple oxides are compared in Figure 7 to those presented in Figure 6. It is obvious from Figure 7 that the peaks emitted from alkaline earth metal oxides (Be,

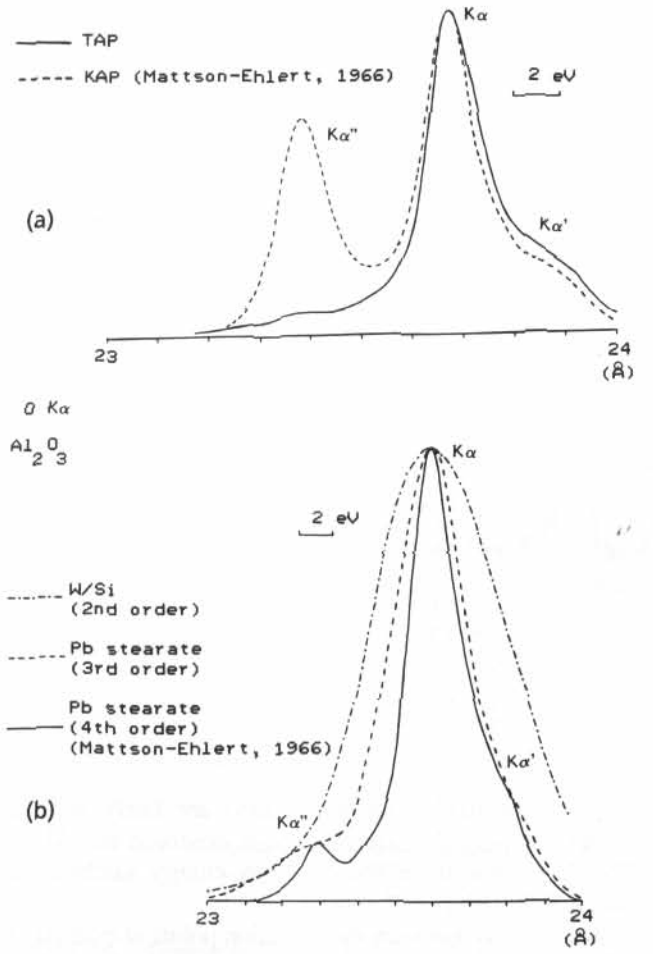

FIGURE 12. Oxygen emission lines from Al_2O_3 using (a) KAP and TAP, and (b) W/Si multilayer (second order) and lead stearate (third and fourth order).

Mg, Ca, Ba) are narrow compared to the others. SiO_2 and Al_2O_3 show peaks with similar FWHM, close to that of Cu_2O.

The O Kα peaks emitted from MgO and Fe_2O_3 are compared in Figure 8a. For MgO, the low-energy satellite forms a pronounced hump on the main peak, whereas K$\alpha_{3,4}$ appears as a shoulder on the high-energy side at less than 2 eV from the peak maximum. No shift is noted for these two peaks. Following Holliday (1968), the number of valence electrons transferred to oxygen atoms should be unchanged for both specimens. One should also note the large difference in FWHM. This last point could be explained by the hybridization of O states with cation valence states, which are broader for Fe than for Mg (Kefi *et al.*, 1993).

Results for oxygen EPMA in MgO with Fe_2O_3 as the standard are plotted in Figure 8b. The experimental area k-ratios are systematically overestimated by 10–11%, compared to the calculated ones over the accelerating-voltage range. This could be a clear illustration of the influence of changes in the matrix element r_{if} (as has been discussed in the introduction) on the generated intensity. The broader the peak is, the lower r_{if} will be, and, finally, the less intense the X-ray emission will be.

Figure 9 presents results similar to those in Figure 8 for MgO and BeO. Both peaks are now similar in position and in shape, reflecting no strong changes in the oxygen atoms' environment for both specimens, and no EPMA anomaly is noted.

Clearly, a relationship between the position and the shape of the O Kα peak (as resolved by a monochromator with a high enough resolving power) must be satisfied in order to obtain accurate results with EPMA. Peaks that belong to the hatched region in Figure 7 satisfy this relationship (in particular SiO_2).

However, for this specimen, oxygen contents are overestimated by 7–8% regardless of the chosen operating conditions. The same is true for Al_2O_3, whose peak falls slightly outside the hatched region. This new aspect of the problem is discussed in the next section with the example of Al_2O_3.

Contribution of Bandgap States to the O Kα Peak

In this section, both TAP and lead-stearate monochromators were used for the spectroscopic study of O Kα. Figure 10 shows that although the resolution is better for TAP, the main features of both Ga_2O_3 and Cu_2O spectra are still observed with the lead stearate used in the third order of reflection. The O Kα peaks emitted from Ga_2O_3 and Al_2O_3 are compared in Figure 11, as resolved by lead stearate. Both peaks are similar in shape, except on the high-energy side where a structure (particularly well-shown with lead stearate) appears at 7 to 8 eV from the Al_2O_3 peak maximum. According to a very recent study on α- and γ-Al_2O_3 (Kefi *et al.*, 1993), this peak could result from the contribution to O Kα of defect states present in the specimen bandgap.

First, the spectral response in the O Kα spectrum region must be examined. Indeed, this response depends on the monochromator used. Figure 12a shows extreme spectra obtained with two monochromator crystals of the acid-phthalate series, KAP (Mattson and Ehlert, 1966) and TAP. The weight of the high-energy peak, labelled Kα'', is close to 50% of the total peak for KAP and is reduced some percentage points for TAP. The latter authors have examined the influence of other acid-phthalate monochromators on the ratio of high energy to main peaks intensity.

These spectra illustrate a well-known phenomenon related to the reflectivity anomalies of monochromators containing oxygen, particularly acid phthalate crystals, under Bragg conditions in the region of the O K-absorption edge (532 eV). Bodeur and Barchewitz (1984) have shown that the reflectivity anomalies for KAP may be

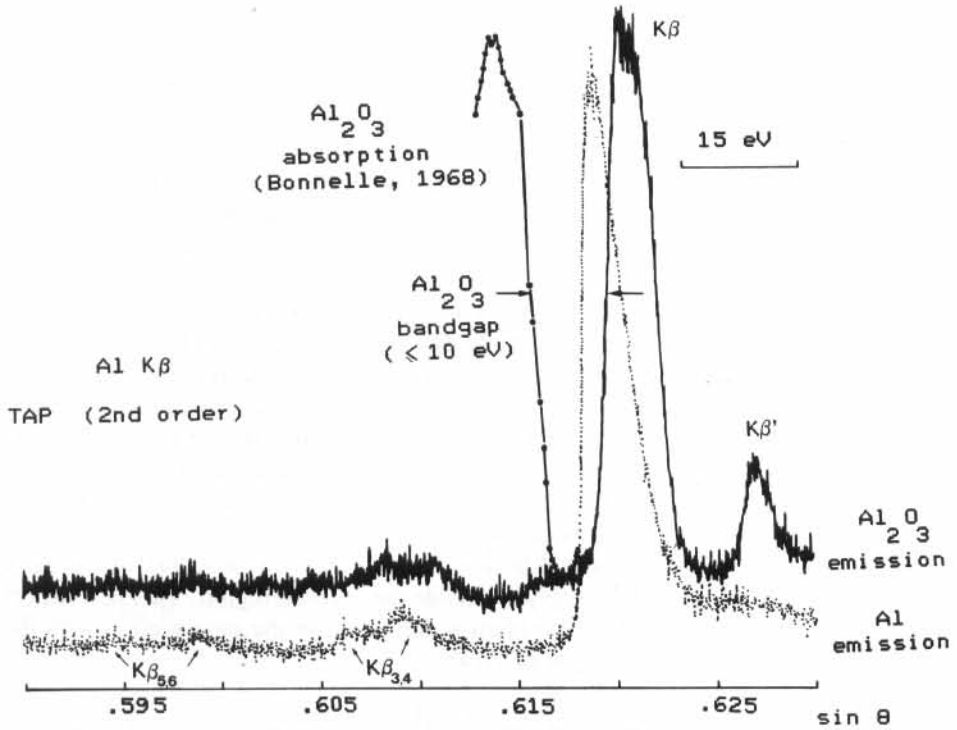

FIGURE 13. Al Kβ spectra from pure Al and Al_2O_3 using TAP (2nd order). Also plotted the absorption spectrum from Al_2O_3 (adapted from Bonnelle, 1968).

correlated with structures in the transmitted-absorption spectrum of the crystal obtained over the O *K*-edge region.

Experiments with oxygen-free monochromators, such as W/Si multilayers, were attempted in order to obtain the true contribution of the high-energy peak to the total peak. Unfortunately, because of the low resolution of these monochromators, no structure has been revealed on the high-energy side of the peak, even in the second order of reflection, the highest order significantly reflected by such crystals (Figure 12b). On the other hand, spectra recorders in the third and fourth order of lead stearate, which contains oxygen, provide valuable information bearing on the problem. Indeed, reflectivity anomalies are expected to strongly change with the order of reflection. Figure 12b shows that, except for the gain of resolution obtained with the fourth-order record, the shapes of both spectra are similar. These measurements constitute an indirect argument in favor of lead stearate, and we conclude that no significant artifact alters the reflectivity of this monochromator.

In order to confirm the contribution of bandgap states to O Kα in Al_2O_3, we have examined the Al Kβ peak, which originates from Al valence orbitals strongly mixed with O orbitals contributing to O Kα. The raw Al Kβ spectra of Al_2O_3 and pure Al are plotted in Figure 13, along with the Al_2O_3-absorption spectrum (Sénémaud, 1966; Bonnelle, 1968). The general features observed include the following: the main Al_2O_3 peak is shifted by −5 eV from that of pure Al. The shake-off peak doublets, $K\beta_{3,4}$ and $K\beta_{5,6}$ (the homologous peaks of $K\alpha_{3,4}$ and $K\alpha_{5,6}$, respectively, for Kα peaks) are fairly well-resolved for pure Al. They are also observed for Al_2O_3. The Al_2O_3 spectrum shows a low-energy satellite, labelled Kβ′.

The distance between the inflection points of both Al_2O_3 emission and absorption curves gives an estimate of the bandgap width of the compound, around 10 eV. The smoothed-Al_2O_3 and pure-Al spectra are compared in Figure 14. Obviously, the peak labelled Kβ″, which extends over the energy range of the Al_2O_3 bandgap, is not present in the pure-Al spectrum.

The origin of all components of both O Kα and Al Kβ peaks emitted from Al_2O_3 are schematically summarized in Figure 15 according to the results of Kefi *et al.* (1993). The high-energy peaks of both O Kα (Kα″) and Al Kβ (Kβ″) correspond to radiative recombination from states located in the bandgap to, respectively, O 1*s* and Al 1*s* vacancies. Kβ′ results from the mixing of Al 3*p* with O 2*s* states to form a part of the Al-O chemical bonds. Correctively, Kα′ is composed of mixed Al 3*sp* and O 2*p* states.

This hybridized peak shows that the expected electron transfer from cation to oxygen is directed from Al 3*sp* to O 2*p* states. Urch (1970) has estimated this transfer to be half an electron. In a previous study of oxygen (Fialin and Remond, 1993), we had suggested that the excess of 0.5 electron on the O 2*p* levels could exactly reflect the increase in O Kα intensity observed for Al_2O_3 with EPMA. In consideration to the arguments that have been discussed in the previous paragraph, this early interpretation is valid if shake-off peaks

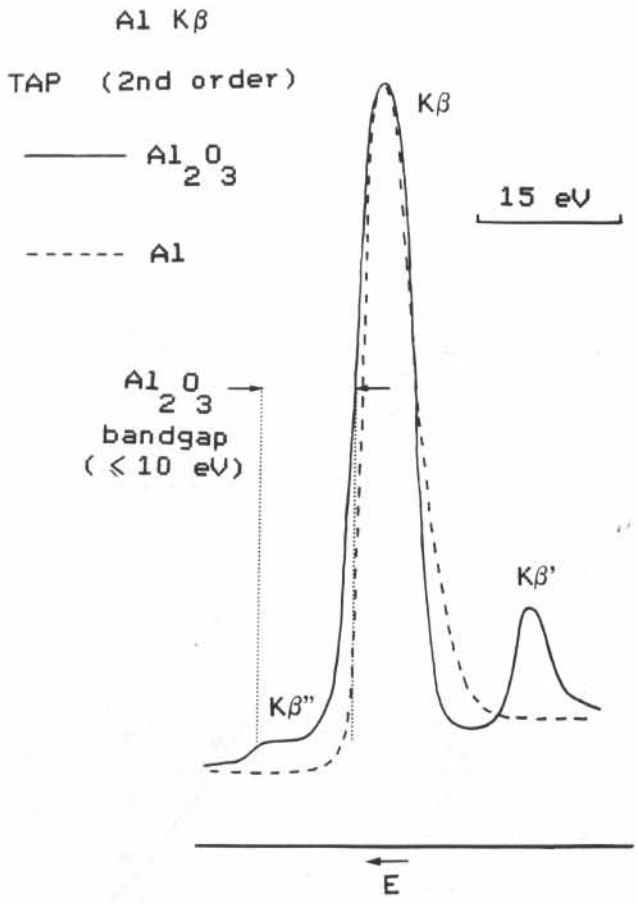

FIGURE 14. Comparison of the shapes of Al Kβ from pure Al and Al_2O_3.

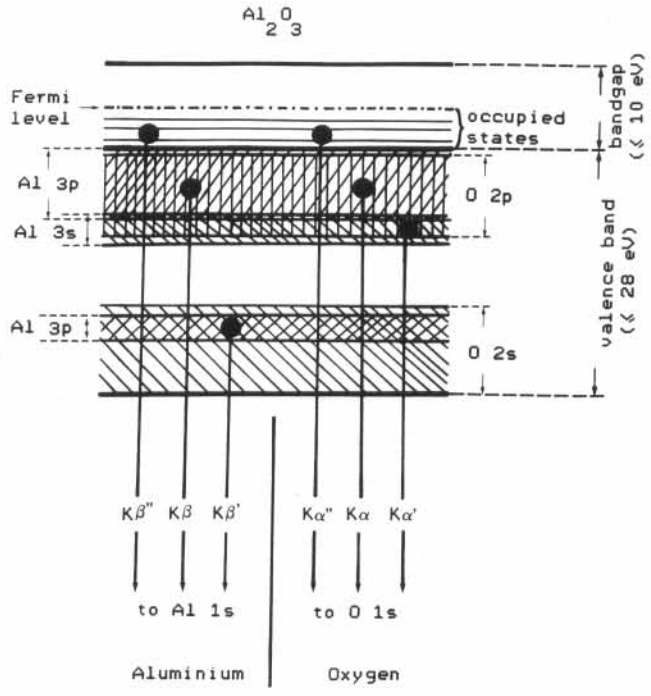

FIGURE 15. Schematic representation of the band structure of Al_2O_3 according to the calculations of Kefi *et al.* (1993). The origin of all components of oxygen and aluminium emission lines are shown.

give no contribution to O Kα. Although these peaks are not observed for Al_2O_3, they may exist very close to the main peak.

Another interpretation is based on the origin of the Kα″ peak. As mentioned previously, this peak results from the radiative reorganization of bandgap states consecutive to the ionization of O 1*s* levels. In particular, this concerns those states that are filled with incident beam electrons, leading to the well-known charging phenomena in insulating materials under irradiation. A study of the charge buildup under irradiation in Al_2O_3 is in progress (Vergand *et al.*, 1994). These recombination processes differ from the conventional processes, radiative or Auger, for which only states of the oxygen atom are involved.

Considering that these processes involve an electron density (the trapped beam electrons) that is not representative of the properties of the local DOS on oxygen atoms, Kα″ can be taken as an almost parasite radiation to be removed from the Kα peak for EPMA applications. The weight of Kα″ is estimated around 7% of the total peak for Al_2O_3, after measurements on spectra recorded with lead stearate and TAP (Figure 16); the anomalous reflectivity of TAP is weak, at less than 1 or 2% (Kefi *et al.*, 1993). Electron probe microanalysis results for Al_2O_3, with Fe_2O_3 as the standard, are presented in Figure 17. Experimental points are plotted with and without Kα″. For the latter, a good agreement with the theoretical curve is obtained.

Kα″ is expected to be close to the O Kα peak for most wide-bandgap oxides and also close to other soft K peaks emitted from large-bandgap compounds. Figure 18 shows the B Kα peak emitted from B_2O_3 (bandgap width = 7 eV). The three characteristic peaks described above (Kα, Kα′, Kα″) for O Kα are fairly well-resolved in both spectra presented (Jacob *et al.*, 1968; Pouchou and Pichoir, 1985).

4. CONCLUSION

As a general conclusion to the study of oxygen EPMA, including a previous article (Fialin and Remond, 1993), we shall list the points to be carefully considered when an analytical anomaly occurs.

1. The error varies continuously, and in general increases, with increasing accelerating voltage. The mass absorption coefficient (m.a.c.) for O Kα in one or several companion elements must be suspected. For

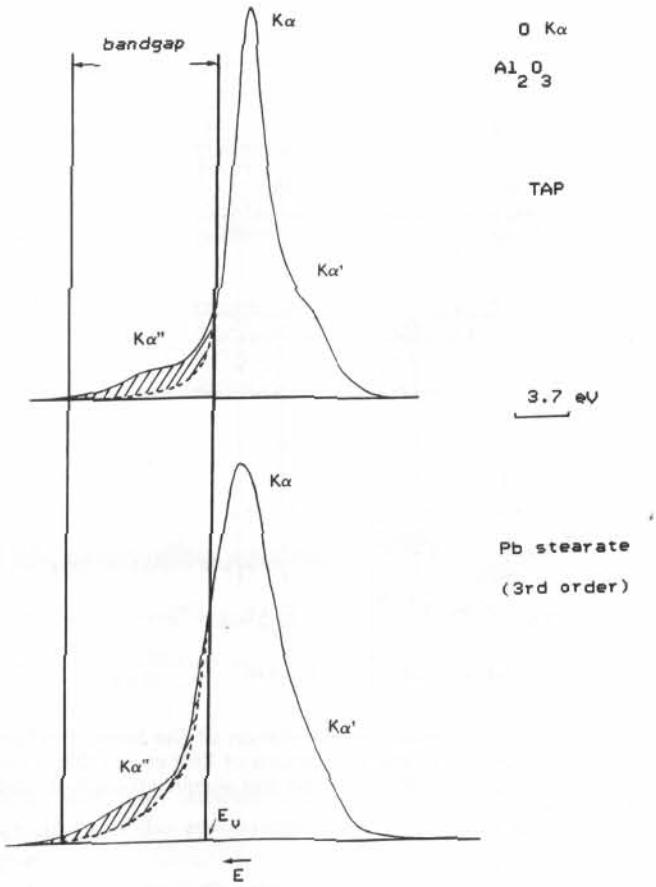

FIGURE 16. Oxygen emission lines from Al_2O_3 using TAP (top) and lead stearate (bottom). E_v is the position of the top of the valence band according to Kefi *et al.* (1993). Hatched areas are estimations of the contribution of bandgap states: around 7% of the total peak in both cases.

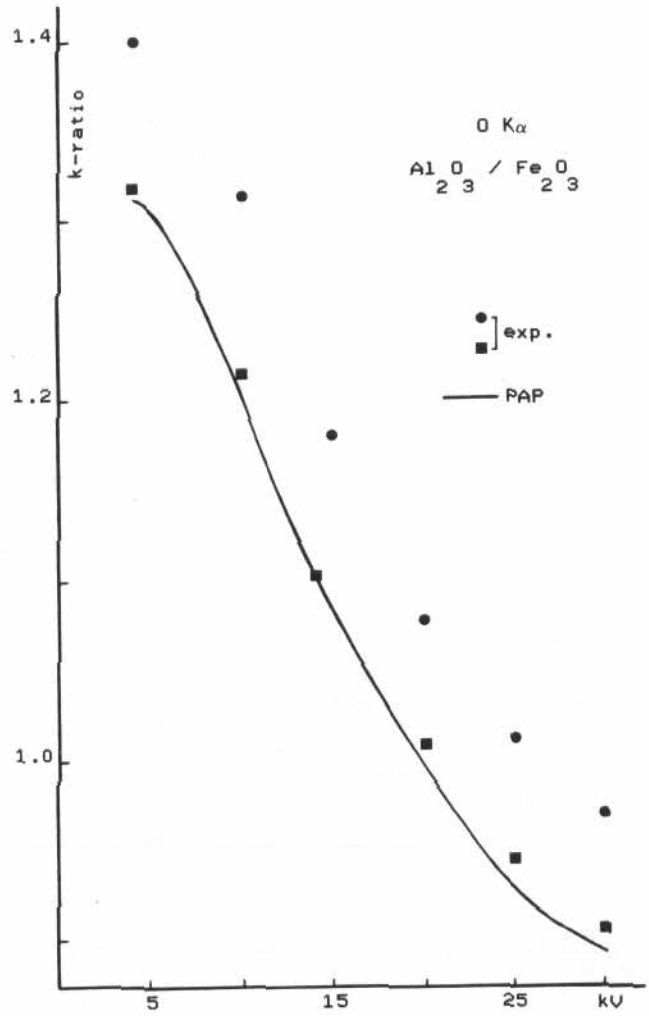

FIGURE 17. O Kα *k*-ratios for Al_2O_3/Fe_2O_3. Experimental points are plotted with (circles) and without (squares) the contribution of the parasite peak Kα".

instance, the O Kα m.a.c. in Ti has been found to be 19900 cm^2/g by Bastin and Heijligers (1989), a value confirmed by our measurements, instead of 22100 cm^2/g according to the Henke *et al.*'s tables (1982), which are the most widely used for light-element analysis. Indeed, O Kα is located very close to the Ti L_1 absorption edge, which renders doubtful the tabulated m.a.c.. The same is true for O Kα located between and very close to both Sn M_{IV} and M_V edges (m.a.c. in Sn ≈ 15050 cm^2/g measured instead of 23100 cm^2/g tabulated). Other examples are found in Bastin and Heijligers (1989) and Fialin and Remond (1993).

2. The error remains constant over a wide range of accelerating voltages. A spectroscopic study of O Kα based on well-resolved spectra is necessary to detect eventual anomalies in the generated intensity, I_{if}, between the unknown and the standard. This was the scope of the present paper. The value of I_{if} strongly depends on the local DOS, the changes of which affect both the peak position, reflecting changes in the density of valence electrons D_f on each atom site, and the peak shape, reflecting changes in the matrix element r_{if}. The role of the shake-off peaks in the total Kα intensity generated is of great importance. For wide-bandgap oxides, a great source of error stems from the contribution of bandgap states in the atomic de-excitation processes.

To complete these remarks, the case of insulating oxides should be briefly examined. This aspect of the problem has been fully discussed in our previous paper. The first step in the analytical procedure of insulators concerns the choice of the nature and the thickness of the conductive surface film to be deposited in order to restore the electrical conductivity. One must be aware of the strong errors induced by an improper film. The example of copper films deposited on oxides (Bastin and Heijligers, 1989) is particularly significant in this respect. For such situations, the film + specimen system can no longer be regarded as a

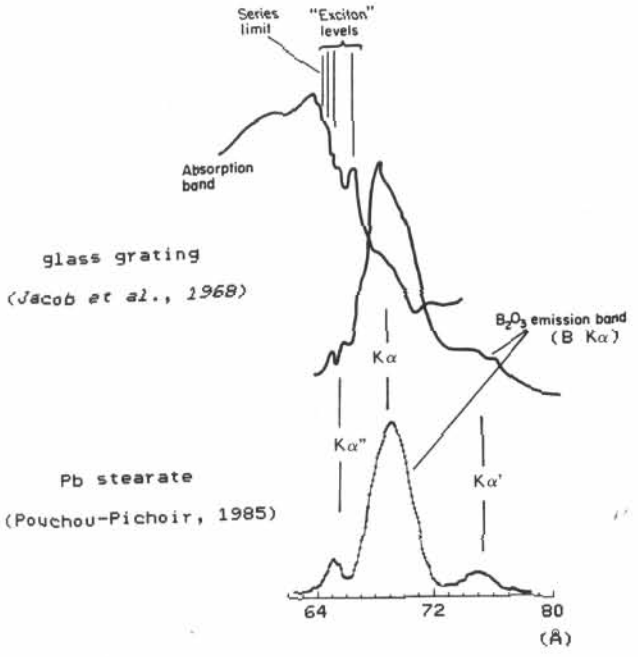

FIGURE 18. Top: B_2O_3 emission and absorption bands resolved by a concave glass grating with three 10^4 lines per inch (Jacob *et al.*, 1968). The contribution of bandgap states, called "exciton" levels, to B Kα is clearly shown. Bottom: B_2O_3 emission band using lead stearate after Pouchou and Pichoir (1985).

bulk-specimen problem; it is a layered specimen, to be treated with proper analytical tools. On the other hand, carbon films, 15 to 20 nm thick, are almost neutral from this point of view.

Another source of errors could arise from the influence of the insulating nature of the specimen on the generated X-ray emission. A model of beam-induced electric field has been proposed by Cazaux (1986) as a valuable attempt to describe the complex phenomena related to the electronic bombardment of insulators. This field is expected to modify the trajectory of the ionizing electrons within the specimen (i.e., the depth distribution function $\phi(\rho z)$) (Kotera and Suga, 1988). Nevertheless, evidence for anomalies in low-Z EPMA, expected under these conditions, is yet to be clearly established.

5. ACKNOWLEDGEMENT

Thanks to Michel Outrequin (CAMECA, France) for the records of O Kα spectra with TAP. For G. Remond, this is the BRGM contribution No. 94027; this work was financially supported by a BRGM research project.

REFERENCES

Aberg, T., "Theory of X-ray Satellites," Phys. Rev., 156 (1), (1967), 35–41.

Bastin, G. F. and Heijligers, H. J. M., "Quantitative Electron Probe Microanalysis of Carbon in Binary Carbides," Internal Report, Eindhoven University of Technology, Eindhoven, Netherlands, 1985.

Bastin, G. F. and Heijligers, H. J. M., "Quantitative Electron Probe Microanalysis of Boron in Binary Borides," Internal Report, Eindhoven University of Technology, Eindhoven, Netherlands, 1986.

Bastin, G. F. and Heijligers, H. J. M., "Quantitative Electron Probe Microanalysis of Oxygen," Internal Report, Eindhoven University of Technology, Eindhoven, Netherlands, 1989.

Bastin, G. F. and Heijligers, H. J. M., "Quantitative Electron Probe Microanalysis of Nitrogen," *Scanning*, 13, (1991), 325–342.

Bodeur, S. and Barchewitz, R., "X-ray Reflectivity and Photoabsorption of KAP in the O-K region," *Solid State Comm.*, 49 (1), (1984), 11–13.

Bonnelle, C., "X-ray Spectroscopy," in Annual Report C, The Royal Society of Chemistry, London, (1987), pp. 201–272.

Bonnelle, C., "X-ray Spectroscopy," in *Physical Methods in Advanced Inorganic Chemistry*, H. A. O. Hill and P. Day, Eds., Interscience Publisher, 1968, p. 45.

Cazaux, J., "Some Considerations on the Electric Field in Insulators by Electron Bombardment," *J. Appl. Phys.*, 55, (1986), 1418–1430.

Feldman, L. C. and Mayer, J. W., *Fundamentals of Surface and Thin Film Analysis*, North-Holland, New-York, 1986.

Fialin, M. and Remond, G., "Electron Probe Microanalysis of Oxygen in Strongly Insulating Oxides," *Microbeam Anal.*, 2, (1993) 179–189.

Fialin, M., Henoc J., and Remond G., "A Survey of Electron Probe Microanalysis using Soft Radiations: Difficulties and Presentation of a New Computer Program for WDS," to be published as Supplement 7 Scanning Microscopy, 1993.

Fischer, W., "Effect of Chemical Combination on the X-ray Emission Spectra of Oxygen and Fluorine," *J. Chem. Phys.*, 42 (11), (1965), 3814–3821.

Henke, B. L., Lee, P., Tanaka, T. J., Shimabukuro, R. L., and Fujikawa, B. K., "Low-energy X-ray Interaction Coefficients: Absorption, Scattering and Reflection," *Atomic Data and Nuclear Data Tables*, 27, (1982) 1–144.

Holliday, J. E., "Soft X-ray Emission Bands and Bonding for Transition Metals, Solutions and Compounds," *in Soft X-ray Band Spectra*, D. J. Fabian, Ed., Academic Press, New York, 1968, p. 101.

Jacob, L., Noble, R., Yee, H., and Fraenkel, B., "K-Absorption of Boron in Boron Trioxide," in *Soft X-ray Band Spectra*, D. J. Fabian, Ed., Academic Press, New York, 1968, p. 81.

Kefi, M., Jonnard, P., Vergand, F., Bonnelle, C., and Gillet, P., "Hybridization of Al and O states in α and γ–alumina," *J. Phys.: Condens. Mat.*, 5, (1993), 8629–8642.

Kotera, M. and Suga, H., "A Simulation of keV Electron Scatterings in a Charged-up Specimen," *J. Appl. Phys.*, 63 (2), (1988), 261–268.

Mattson, R. A. and Ehlert, R. C., "The Application of a Soft X-ray Spectrometer to Study the Oxygen and Fluorine Emission Lines from Oxides and Fluorides," *Adv. X-ray Anal.*, 9, (1966), 471–486.

Pouchou, J. L. and Pichoir, F., "Détermination par Microan-

alyse X de l'Epaisseur et de la Composition des Couches Minces Superficielles," *J. Microsc. Spectrosc. Electron.*, 10, (1985), 279–290.

Remond, G., Coutures, P., Gilles, C., and Massiot, D., "Analytical Description of X-ray Peaks: Application to L X-ray Spectra Processing of Lanthanide Elements by Means of the Electron Probe Micro-Analyzer," *Scanning Microsc.*, 3 (4), (1989), 1059–1086.

Sénémaud, C., "Etude par Spectroscopie X de la distribution des niveaux électroniques de Paluminium dans le métal et dans l'oxyde Al_2O_3," *J. Physique*, Supp. 27, (1966), 2–55.

Urch, D. S., "The Origin and Intensities of Low Energy Satellites Lines in X-ray Emission Spectra: A Molecular Orbital Interpretation," *J. Phys. C: Solid St. Phys.*, 3, (1970), 1275–1291.

Vergand, F., Kélí, M., Jonnard, P., and Bonnelle, C., unpublished research.